Flame structure of ethanol-air premixed mixtures at high pressures in microgravity

M. Nassouri, C. Chauveau, F. Halter, I. Gökalp

Flame structure of ethanol-air premixed mixtures at high pressures in microgravity

M. Nassouri*[1], C. Chauveau[1], F. Halter[1,2], I. Gökalp[1]

[1] Institut de Combustion, Aérothermique, Réactivité et Environnement (ICARE), CNRS-INSIS, Orléans, France

[2] Laboratoire PRISME, University of Orléans, France

Abstract

The objective of the present research is the experimental determination of the flame structure for both droplet-vapor-air and vapor-air mixtures. The effects of initial conditions and the smallest fuel droplets on the flame structure and cell formation are particularly investigated. Idealization of spray configurations in a quiescent environment has been impossible in normal gravity with droplet-vapor-air mixtures due to the settling of large droplets. Therefore, the experiments were conducted for initial pressures up to 9 bars, both in normal and microgravity conditions. The experimental equipment is designed to be used aboard the Airbus A300-0g of the CNES. The results obtained allowed determining the effects of the gravity on the flame behavior for both vapor-air and droplet-vapor-air mixtures. The effect of drop concentrations on the flame structure is also investigated. Experimental results reveal that the pressure and the equivalence ratio are the most dominant parameters in terms of the onset of flame instability for the vapor-air mixtures.

Introduction

Towards the challenge concerning rarefaction of fossil energies, and in a durable developmental perspective, it is essential to very strongly invest in the control of energy consumption's and the emergence of new technologies making it possible to better exploit renewable energies. This study aims at looking further into knowledge on the phenomena concerned during the combustion of liquid fuels dispersed as aerosol. Two-phase combustion is a widespread mechanism of energy conversion that is of practical importance in gas turbines, diesel and spark ignition engines, furnaces, and hazardous environments.

Recent studies showed that the flames being propagated through an aerosol/vapor mixture could show characteristics extremely different from their counterparts premixed gas (flame propagation velocity increased, inflammability limits extended). These characteristics can have advantages for certain applications (engines…) but also disadvantages for other cases such as those met in the context of the industrial risks. Thus, an understanding of the influence of the presence of liquid drops in a laminar aerosol flame is essential. Many studies were devoted under investigation of the flame propagation in a gas mixture, for various conditions of pressures and temperature, and for many fuels. Those devoted to the flame propagation in an aerosol/vapor mixture are sparser. Consequently, there are few experimental data of a fundamental nature which clearly shows the similarities and the differences for the laminar burning velocity between single and two phase combustion.

In this paper, spherical expanding flames are used to measure the differences in the structure of instabilities in laminar gaseous and aerosol flames. Aerosols of ethanol/air, in the droplet size range of 10 µm, are formed by the expansion of a gaseous pre-mixture to produce a homogeneous suspension of fuel droplets. The use of reduced gravity conditions, thanks to parabolic flights, made it possible to reduce the effects of the sedimentation of the droplets, and to be freed from the effects of the buoyancy on the propagation of the very slow flames.

Objectives

The first step of our work was to characterize experimentally the size of droplets composing the aerosol. This investigation was performed using a laser diffraction particle size analyzer. Aerosol mixtures are generated by the condensation by expansion cooling technique (Wilson cloud chamber technique), using ethanol as fuel. Under reduced gravity conditions larger droplet sizes are obtained together with more homogeneous and more mono-disperse aerosol mixtures [1].

During the second step, studies of the propagation of the spherically expanding flames have been performed, for the previously characterized mixtures. Imaging is used to observe the propagation of the flame. Several initials conditions were varied such as pressure and the total equivalence ratio. Spherical flames were generated for both fuel droplet-vapor-air mixtures and premixed gas mixtures. The effects of droplet size distribution on the flame speed and structure have been investigated. The most recent similar studies were carried out by Lawes [2] using isooctane fuel in normal gravity condition and Nomura [3] using ethanol fuel in microgravity condition.

Experimental apparatus and procedure

Experiments were conducted in a dual-chamber pressure release type high-pressure combustion apparatus shown in Figure 1. The combustion chamber consists of a cylindrical vessel of 82.5 mm inner

* Corresponding author: mouhannad.nassouri@cnrs-orleans.fr

diameter, and 110 mm length. This inner vessel is located concentrically in an octagonal high pressure chamber able to sustain up to 12 MPa. This outer chamber is filled with nitrogen gas at same pressure as the inflammable mixture introduced in the inner vessel. Six specific pressure relief valves with 7 mm outlet diameter are located in the radial wall of the inner vessel symmetrically from the centre and angularly at 0, 120, and 240 degrees to allow for pressure release. The relief valves, equipped with calibrated compression spring, provide a seal between chambers for pressure differences between inner and outer chambers less than 0.5 atm. When the pressure difference exceed, the valves open allowing gases to flow from the inner to the outer chamber to maintain a nearly constant pressure. Since the inner vessel volume is 10 times smaller than that of the outer one, the total pressure increase after combustion is small, ensuring not only a nearly constant-pressure experiment, but operational safety for experiments conducted at high initial unburned gas pressures. Optical access is obtained through a pair of windows of 60 mm usable diameter, disposed face to face. The maximum allowed initial temperature of the inner vessel is 150 °C ensured jointly by heating cables, thermocouples and a PID regulator.

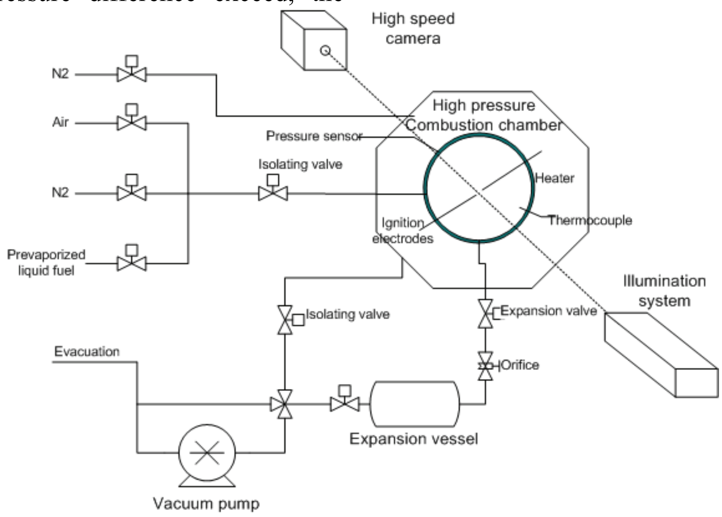

Fig. 1. Schematic representation of the combustion apparatus

Before filling a vacuum is created inside the chamber. The gases (air: inner, N_2: outer) are introduced into the dual-chamber with thermal mass flow meters. The fuel is regulated thanks to a sample loop connected to the air injection. The use of a sampling and switching valve allows multiple injections of liquid with accuracy. The liquid fuel pushed by the air is then vaporized and mixed before being introduced into the combustion chamber. The mixture is ignited by two electrodes which form a spark in the centre of the combustion chamber. Although the capacitive discharge ignition system makes it possible to vary the deposited energy, the results presented in this paper are obtained with fixed adjustments of the ignition system.

A FrontDaq acquisition system is used to record the outputs of the system (pressure, temperature), whereas the whole control of the experiment, like specifying and monitoring the mixture preparation process, is ensured by a “Siemens Simatic” automation controller. A shadow photography system allows imaging of the flame front for a diameter up to 50 mm. Illumination is provided by a laser-driven light source (Energetiq); the parallel light beam is created by using two planoconvex lenses.

The evolution of the flame surface development is observed from shadowgraphy images recorded with a high speed CMOS Phantom v1210 camera operating at 15000 frames/s. The number of images considered in all experiments is higher than 200.

Results and Discussion

Ethanol-Air mixtures in microgravity

In normal gravity the droplets rapidly settle which increases the droplets number density N (droplets number/m^3) in the lower part of the combustion chamber and decreases it in the upper part. This produces an asymmetric structure of the flame and also disrupts its sphericity.

Figure 2 shows different behaviors of the flame in normal gravity and microgravity conditions. It was shown in the literature that the presence of droplets in a vapor-air mixture changes the flame structure, Hayashi [4] proposed that the presence of droplets produces heterogeneity in the unburned mixture, which should be responsible for the initiation process of such roughened cellular flame fronts and that the development of the roughness must be associated with the instability of the flame front. The pictures show that the roughness of the flame front increases as the flame ball grows.

Figure 2.A shows the effect of droplets on the flame structure at the same initial conditions in normal gravity and in microgravity. The effect of droplet sedimentation on the flame structure can be clearly observed as the cellular structure in normal gravity is concentrated in the lower part of the flame, whereas in the upper part which only includes a vapor-air mixture, no cellular structures are observed.

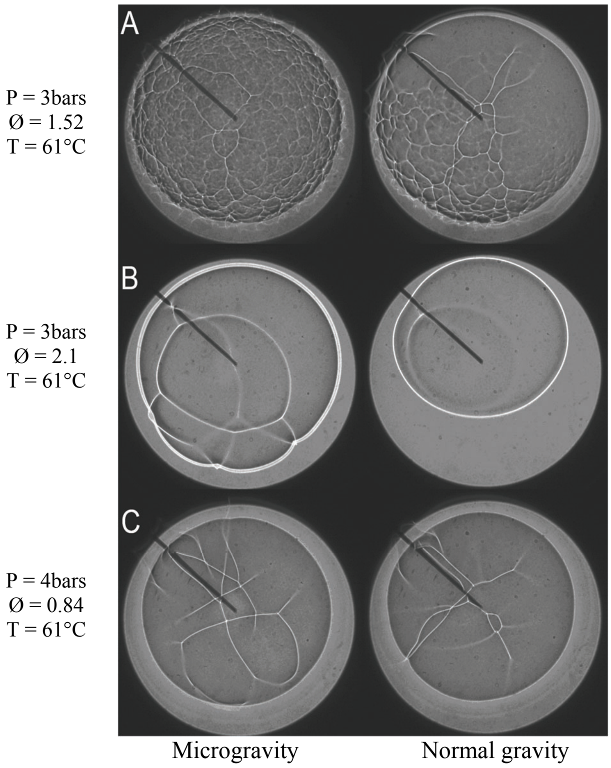

Fig. 2. Images of ethanol droplet-vapor-air mixture flames

Figure 2.B shows the effect of microgravity on the flame behavior for rich vapor-air mixtures. The flame propagates slowly, and due to buoyancy, the flame balls have tendency to rise up. However for equivalence ratio values between 0.75 and 1.6, this phenomenon is rarely observed, as one can notice it on Figure 2.C. For high equivalence ratio, the presence of droplets can change a non-flammable vapor-air mixture to a flammable droplet-vapor-air mixture.

Figure 3 shows various flames which were ignited at the same initial conditions of pressure, temperature and equivalence ratios, but at various moments after the end of the expansion. Droplet evaporation rates (which depends on the initial temperature and pressure as our previous study has showed [1]) determine the duration of the aerosol lifetime before its complete vaporization. After the end of expansion time (which is 1.5s in our case) the droplet-vapor-air mixture is becoming more and more dilute with time passing, until the moment when the droplets are completely evaporated and then only a vapor-air-mixture exists. Figure 3 shows droplet sedimentation due to gravity. Experiences show that sedimentation starts 1sec after the end of the expansion and then a high concentration of small cells in the lower part of the flame is observed. The cells become larger in the upper part, until the moment when the cells disappear and the flame structure becomes that of a vapor-air mixture.

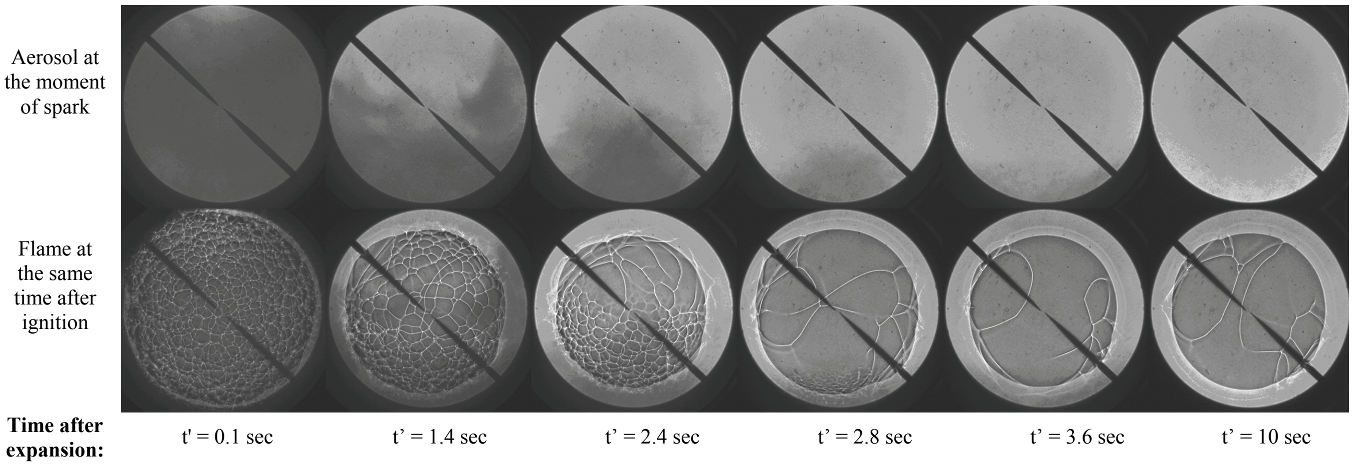

Fig. 3. Flame structures of ethanol-air mixtures at 60 °C, 4 bars and Ø=1.56
All pictures are taken at 1.1ms after the flame ignition.

Flame structure and instability

During the investigation of spherical flames, two categories of instabilities are observed: unequal diffusion instability caused by unequal mass and thermal diffusion rates, and hydrodynamic instability caused by interactions between the flame and external disturbances. Many studies were devoted to the cells formation and the onset of instability in homogeneous vapor-air mixtures such as Bradley [5, 6], Gu [7], Jomaas [8], Liu [9], Eisazadeh-Far [10, 11], and Marshall [12]. However, studies on cellular instabilities in droplet-vapor-air mixtures are scarcer. Pioneering works of Atzler [13] and Nomura [14] are references on the effects of the fine droplets on the laminar flame speed.

Figure 4 shows the evolution of instabilities at the same initial conditions of pressure, temperature and equivalence ratio, for vapor-air mixtures and droplet-vapor-air mixtures. It can be noticed that until 5ms after flame initiation, there is no notable effect of droplets. However for later times, we dramatically note the droplet effect in droplet-vapor-air mixtures where we observe a significant multiplication of the cell number by scissiparity while the number of cells in vapor-air mixture remains sensibly the same. To better understand these differences, we studied the two types of mixture separately.

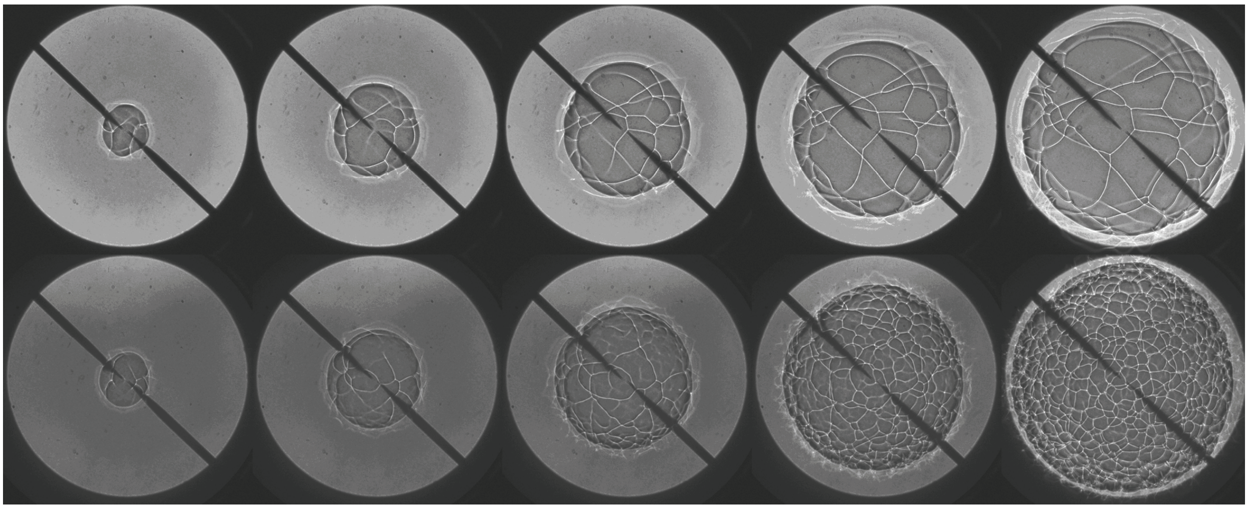

Fig. 4. Flame structure of ethanol/air mixtures at 60 °C, 3.2 bars and Ø=1.52, both for gas and aerosol mixtures.

a. <u>Flame structure of Droplet-Vapor-Air mixtures</u>

Chiu [15] had already attempted to classify the different possible structures of droplet-vapor-air mixture flames, depending of the total number of droplets and the group combustion number G, which is mainly based on R_e and P_r numbers (Reynolds and Prandtl numbers respectively). Borghi [16] has also discussed the same problem by considering two non-dimensional parameters: d_g/e_L, the ratio of the mean initial droplet diameter to the characteristic thickness of a laminar flame, and $n^{1/3}.r_F$, where n is the droplet number density (droplets number / m^3), $n^{1/3}$ is the average distance which separates the droplets and r_F is the radius of the diffusion flame that would be established around the mean droplet if it was alone in the oxidizing medium. Borghi [16] has shown that the flame structure will mainly depend on the droplets spacing parameter ($\mathbf{n^{1/3}.r_F}$).

When the flame zone approaches an aerosol in which droplets are sufficiently small or the propagation flame speed is sufficiently slow, these droplets may have enough time to fully vaporize. The value of this critical droplet diameter, below which droplets evaporate before the reacting zone, was defined by Hayashi [17]. This critical diameter is above all sensitive to the propagation flame speed. For our cases we consider that the sizes of the fuel droplets are not necessarily identical, but they exhibit a near monosized distribution around a mean diameter value of 7µm; these values were measured during our previous work [1]. We also consider that the medium is stagnant; the position of the fuel droplets is not regularly fixed, but is randomly and homogeneously distributed in microgravity. We shall add that the droplets spacing parameter $n^{1/3}.r_F$ was calculated by considering that the initial quantity of condensed ethanol due to the expansion, is equal to the necessary quantity to achieve the saturated vapor pressure, which was calculated using Antoine equation [18].

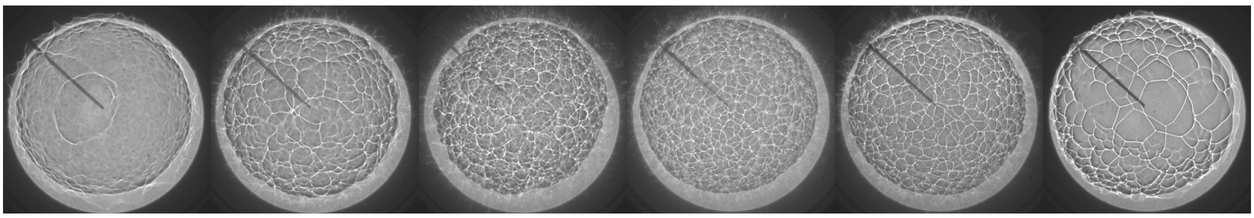

Fig. 5. Flame structure at 61°C, for droplet-vapor-air mixtures in microgravity.

Figure 5 shows that at the same equivalence ratio (ϕ= 0.84) and three different droplet spacing parameters values, we have three different flame structures. The flame in the lean droplet-vapor-air mixtures with a very dilute aerosol (ϕ= 0.84, $n^{1/3}.r_F$ = 0.27) is smoother and the flame front roughness increases with the increasing of droplets spacing parameter values.

However, if we increase the flame propagation speed by increasing equivalence ratio to (ϕ= 1.2) keeping the droplet spacing parameter at ($n^{1/3}.r_F$ = 0.45), no significant change in the flame structure can be noticed. By increasing more the equivalence ratio, a different flame structure with larger cells can be observed. This flame structure was remarked for all rich droplet-vapor-air mixtures (above ϕ= 1.5), independently of the droplet spacing parameter value.

Figure 3 also shows the effect of droplets concentration on the flame structure. When the flame ignition is at 0.1 s after the expansion a dense cloud of droplets is obtained, which produces a dense cellular flame structure. However, when flame ignition takes place at 1.2 s and 1.4 s, droplet distributions become more dilute and the flame structure smoother.

b. Flame structure of Vapor-Air mixtures

The onset of flame instabilities of laminar ethanol vapor-air spherical premixed flames has been studied in the previously described apparatus, but without expansion. The initial pressures have been varied. Experimental results reveal that the pressure and the equivalence ratio are the most dominant parameters versus among all those studied.

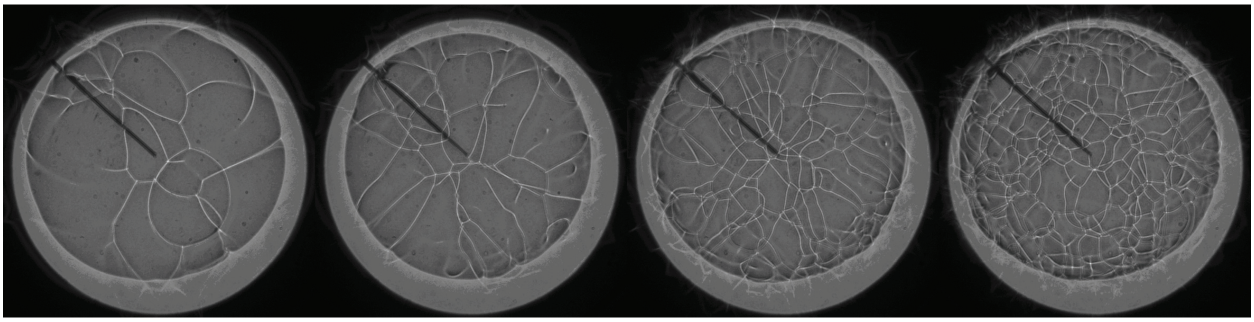

Ø = 0.84 Ø = 1 Ø = 1.2 Ø = 1.4

Fig. 6. Flame structure of ethanol vapor-air mixtures at 5 bars and 61°C

Figure 6 shows 4 vapor-air mixture flames, performed at 5 bars, 61°C and 4 different equivalence ratios. The effect of the equivalence ratio on the unequal diffusion instability can be clearly identified. The instabilities increase with the increasing equivalence ratio.

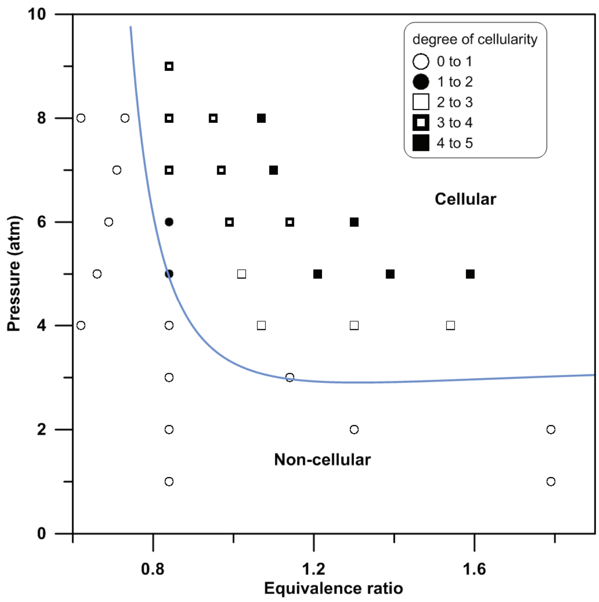

Fig.7. Effect of pressure and equivalence ratio on cell formation

For a better understanding of the observed phenomena, vapor-air mixture flames have been produced by varying the initial pressure from 1 up to 9 bars. For each pressure, the equivalence ratio was varied from 0.6 to 1.7. Figure 7 shows the experimental results obtained where both cellular and non-cellular zones can be identified. For initial pressures less than 3 bars, instabilities are not observed. Starting from 3 bars and Ø = 0.8 instabilities start to show up and become more intense with the increase of both pressure and equivalence ratio. This result is similar to those which have been described by Eisazadeh-Far [11] on the ethanol vapor-air mixture flames. They found that during the pressure increase throughout the flame propagation, cell formation is strongly dependent on the equivalence ratio, and for each equivalence ratios there is a specific range of pressure at which the flame becomes cellular.

Conclusions

The aim of the present work was to characterize the impact of fine droplets on the flame structure and cell formation in an aerosol mixture. Experiments in normal and microgravity conditions are conducted with ethanol as fuel. The effects of initial pressure and global equivalence ratio are investigated. Comparisons between the flame structures of vapor-air mixtures and droplets-vapor-air mixtures have been presented. Settling effects under normal gravity are clearly demonstrated. The use of microgravity conditions extends the experimental domain and allows examining more homogeneous and stable aerosol clouds. For the vapor-air mixtures, gravity does not disturb the flame behavior for an equivalence ratio less than ϕ= 1.5. Concerning the instabilities due to the presence of the droplets in an aerosol, we observe that the droplet spacing parameter ($n^{1/3}.r_F$) is the main factor, except for rich mixtures. It is also highlighted that the increase of the pressure and equivalence ratio intensifies the onset of instability in vapor-air mixtures.

Acknowledgements

The authors greatly acknowledge the continuous support of the CNES and the CNRS through the GDR MFA n°2799. M. Nassouri is supported by a joint grant from the CNES and the Conseil Régional Centre.

References

1. M. Nassouri; C. Chauveau; F. Halter; I. Gökalp in: *Combustion of aerosols: droplet sizing study in microgravity*, ICLASS 2012, 12th Triennial International Conference on Liquid Atomization and Spray Systems, Heidelberg, Germany, September 2-6, 2012.
2. M. Lawes; Y. Lee; N. Marquez, Combustion and Flame 144 (3) (2006) 513-525.
3. H. Nomura; M. Koyama; H. Miyamoto; Y. Ujiie; J. Sato; M. Kono; S. Yoda, Symposium (International) on Combustion 28 (1) (2000) 999-1005.
4. S. Hayashi; S. Kumagai; T. Sakai, Combustion Science and Technology 15 (5-6) (1977) 169-177.
5. D. Bradley, Philosophical Transactions of the Royal Society A: Mathematical, Physical and Engineering Sciences 357 (1764) (1999) 3567-3581.
6. D. Bradley; R. A. Hicks; M. Lawes; C. G. W. Sheppard; R. Woolley, Combustion and Flame 115 (1-2) (1998) 126-144.
7. X. J. Gu; M. Z. Haq; M. Lawes; R. Woolley, Combustion and Flame 121 (1-2) (2000) 41-58.
8. G. Jomaas; C. K. Law; J. K. Bechtold, Journal of Fluid Mechanics 583 (2007) 1-26.
9. F. Liu; X. Bao; J. Gu; R. Chen, International Journal of Hydrogen Energy 37 (15) (2012) 11458-11465.
10. K. Eisazadeh-Far; F. Parsinejad; H. Metghalchi, Fuel 89 (5) (2010) 1041-1049.
11. K. Eisazadeh-Far; A. Moghaddas; J. Al-Mulki; H. Metghalchi, Proceedings of the Combustion Institute 33 (1) (2011) 1021-1027.
12. S. P. Marshall; S. Taylor; C. R. Stone; T. J. Davies; R. F. Cracknell, Combustion and Flame 158 (10) (2011) 1920-1932.
13. F. Atzler; M. Lawes; S. A. Sulaiman; R. Woolley, in: *ICLASS 2006*, Kyoto, Japan, 2006.
14. H. Nomura; M. Hayasaki; Y. Ujiie, Proceedings of the Combustion Institute 31 (2) (2007) 2265-2272.
15. H. H. Chiu; H. Y. Kim; E. J. Croke, Symposium (International) on Combustion 19 (1) (1982) 971-980.
16. R. Borghi, Lecture series - van Kareman Institute for fluid dynamics 2 (1996) I1-I39.
17. S. Hayashi; S. Kumagai, Symposium (International) on Combustion 15 (1) (1975) 445-452.
18. A. Saat; N. Dutta; M. A. Wahid, AIP Conference Proceedings 1440 (1) (2012) 109-115.